Nonlinear Dyn (2016) 85:1791–1804
DOI 10.1007/s11071-016-2795-0

ORIGINAL PAPER

Impact angle constrained guidance for all-aspect interception with function-based finite-time sliding mode control

Yao Zhao · Yongzhi Sheng · Xiangdong Liu

Received: 13 September 2015 / Accepted: 13 April 2016 / Published online: 4 May 2016

Abstract In this paper, the impact angle constrained guidance problem, focusing on the nonlinear engagement dynamics, is considered. In order to fulfill the terminal constraints, a novel function-based finite-time sliding mode control methodology is introduced to design the guidance law. The main feature of this guidance law is that it achieves the desired impact angle exactly at the time of interception. In addition, it is capable of ensuring a continuous and smooth control action. To improve the tolerance of initial heading errors and broaden the application, a feasible guidance logic is also developed. Numerical simulations in various scenarios have shown that the proposed guidance scheme can realize all-aspect interception against stationary, constant-velocity and maneuvering targets. Furthermore, comparison studies with respect to nonsingular terminal sliding mode control-based methods demonstrate the superiority of the proposed method.

Keywords Guidance · Impact angle · Sliding mode control · Finite-time control · All-aspect interception

1 Introduction

The primary objective of terminal guidance is to produce a minimum miss distance between the missile and the target. In current guidance law design, the impact angle constraint is also of paramount importance due to the requirement of enhancing the effect of warhead.

Conventional guidance laws, such as proportional navigation guidance (PNG) [1,2] and its variants [3–7], have been widely used as the guidance scheme in the homing phase because of its ease of mechanization due to less information demand. Apart from PNG, the guidance laws based on modern control theory have also been proposed, such as suboptimal guidance law [8], backstepping guidance law [9] and Lyapunov-based guidance law [10]. These guidance laws were developed based on Lyapunov theory to ensure asymptotic stability or exponential stability. Hence, the line-of-sight (LOS) angular rate converges to zero with infinite settling time.

Finite-time control usually shows superior properties, such as faster convergence rate, higher accuracy and better disturbance attenuation [11]. Therefore, it is important to design finite-time guidance laws for engineering application. In recent years, some valuable contributions in this field have been made [12–22]. In [12], a guidance law based on Lyapunov scalar differential inequality was derived for maneuvering targets using a finite-time stability approach. Afterward, this method was further investigated in [13] taking the autopilot lag into consideration. Although the methods proposed in [12,13] ensure finite-time error convergence, both fail to address the impact angle constraint. The approach proposed in [14] took advantage of the finite-time reaching phase of the sliding mode

Y. Zhao · Y. Sheng (✉) · X. Liu
School of Automation, Beijing Institute of Technology, Beijing 100081, People's Republic of China
e-mail: shengyongzhi@bit.edu.cn

control (SMC) technique to guarantee that the impact angle constraint can be satisfied at the time of interception. But this law is not applicable for the task of hitting a maneuvering target. Based on the finite-time convergence stability theory and the SMC theory, the impact angle control guidance law was developed for intercepting maneuvering targets in [15]. The guidance law in [16], which was obtained through a combination of finite-time sliding mode control theory and generalized disturbance observer, considers the target maneuvers as well as the missile autopilot dynamics. The impact angle in [15,16] was defined as the LOS angle. In terms of enhancing the lethality, the angle between the velocity vectors of the missile and the target at the time of interception is a better choice [17–19]. In [17], terminal sliding mode (TSM) control-based guidance laws, which ensure finite-time convergence to the desired impact angle, for stationary, constant-velocity and maneuvering targets, were proposed. But this approach suffers from singularity problems which may lead to control saturation. To overcome this defect, nonsingular TSM (NTSM) control algorithm was introduced to handle the impact angle control problem in [18]. Note that the target acceleration was crucial for implementing the guidance laws in [17,18], but unfortunately, the obtaining of the target acceleration was not discussed in the aforementioned literature. To deal with this problem, the guidance law in [19] was designed through a combination of NTSM and a linear extended state observer (LESO). In this study, the target acceleration was estimated by the LESO using the current system states. Apart from the impact angle control problem, finite-time control methods have also been applied to solve the impact time control problem and the impact time and angle control problem. Interested readers may refer to [20–22] and the references therein.

The aim of this study is to provide a new approach to the impact angle constrained guidance problem, with which an all-aspect interception can be achieved with smooth missile acceleration. Firstly, a novel concept of function-based finite-time sliding mode control (FBFTSMC) is presented. By incorporating a specific time-varying function in the design of the sliding surface, this control algorithm can realize a global sliding mode (GSM) and drive the system states to zero at a *pre-specified* finite time in the presence of matched uncertainties. Besides, explicit closed-form solutions for the control system can also be obtained. Then, the well-developed control method is applied to the impact angle control law design. The associated sliding surface is designed using the LOS and time-to-go (t_{go}) information. Under the proposed guidance law, the LOS angle error and its derivative would both converge to zero at the final time which implies the desired impact angle can be achieved at the time of interception. Finally, by designing a feasible guidance logic, the missile can be steered to intercept the target at any impact angle, even in the presence of very large initial pointing errors. This property is termed as "all-aspect interception" [17].

With respect to some previously published work, the method proposed in this study makes several contributions in the following aspects. First, the control methods utilized in [12–19] only ensure bounded convergence time. For the proposed method, however, the convergence time is not only finite but also *well known in advance*. In addition, the FBFTSMC algorithm could provide a lot of flexibility in the controller design by choosing different time-varying functions, whereas other finite-time control methods may not possess this feature. Second, large switching gains are required in [17–19] to enforce a sliding mode, which in turn may aggravate the chattering problem [23]. Although some measures have been taken in [17,19] to alleviate chattering, the resultant guidance commands would be discontinuous. The methodology presented in this study belongs to the GSM category. By the virtue of GSM, a relatively small switching gain is applicable and smooth missile acceleration can be achieved [24]. Third, compared with other impact angle control methods which also have explicit t_{go} in the closed-form guidance laws [25,26], the proposed approach can guarantee interception for all states of the missile and the target during the engagement without accurate t_{go} estimation. Finally, while the method in [27] requires two sliding surfaces to realize all-aspect interception, only one sliding surface is needed in this work.

The rest of this paper is organized as follows. In Sect. 2, the problem formulation is described. In Sect. 3, the basic principle of FBFTSMC algorithm is introduced. In Sect. 4, the impact angle constrained guidance laws are designed based on FBFTSMC and a feasible guidance logic is devised to realize all-aspect interception. In Sect. 5, numerical simulations are performed to validate the effectiveness of the proposed guidance laws. In Sect. 6, conclusive remarks are presented.

2 Problem formulation

In this section, a planar engagement between the missile and the target is considered. The engagement geometry is depicted in Fig. 1a, where both the missile and the target are treated as point masses. The missile and the target are assumed to be traveling at constant speeds of V_{M} and V_{T}, their flight path angle is denoted by γ_{M} and γ_{T}, and the corresponding lateral acceleration is defined by a_{M} and a_{T}. The LOS angle and the distance between the missile and target are represented by λ and r, respectively.

The equations of kinematic engagement for this problem can be found in, for instance, [17], which is described in polar coordinate form as follows:

$$\dot{r} = V_{\mathrm{T}}\cos(\gamma_T - \lambda) - V_{\mathrm{M}}\cos(\gamma_M - \lambda) \tag{1}$$

$$\dot{\lambda} = \frac{V_{\mathrm{T}}\sin(\gamma_{\mathrm{T}} - \lambda) - V_{\mathrm{M}}\sin(\gamma_{\mathrm{M}} - \lambda)}{r} \tag{2}$$

$$\dot{\gamma}_M = \frac{a_{\mathrm{M}}}{V_{\mathrm{M}}} \tag{3}$$

$$\dot{\gamma}_T = \frac{a_{\mathrm{T}}}{V_{\mathrm{T}}}. \tag{4}$$

As shown in Fig. 1b, the impact angle θ_{imp} can be calculated as

$$\theta_{\mathrm{imp}} = \gamma_{\mathrm{Tf}} - \gamma_{\mathrm{Mf}} \tag{5}$$

where γ_{Tf} and γ_{Mf} are the flight path angles of the target and the missile when interception occurs.

When the collision course is enforced, the condition

$$V_{\mathrm{M}}\sin(\gamma_{\mathrm{Mf}} - \lambda_{\mathrm{F}}) = V_{\mathrm{T}}\sin(\gamma_{\mathrm{Tf}} - \lambda_{\mathrm{F}}) \tag{6}$$

holds, which implies the relative velocity perpendicular to the LOS is zero. Similar to [17–19], it is assumed that $V_{\mathrm{T}} < V_{\mathrm{M}}$. Under this assumption, the desired final LOS angle λ_F can be obtained as

$$\lambda_{\mathrm{F}} = \gamma_{\mathrm{Tf}} - \tan^{-1}\left(\frac{\sin\theta_{\mathrm{imp}}}{\cos\theta_{\mathrm{imp}} - V_{\mathrm{T}}/V_{\mathrm{M}}}\right). \tag{7}$$

From Eq. (7), the one-to-one correspondence between λ_{F} and θ_{imp} can be established. The interested reader can refer to [17] for detailed information.

Note that for the maneuvering target case, the target's flight path angle γ_{T} varies with time. In order to ensure a desired impact angle at the time of interception, γ_{Tf}, in Eq. (7), is replaced by its instantaneous value, γ_{T}, which yields [19]

$$\lambda_{\mathrm{F}} = \gamma_T - \tan^{-1}\left(\frac{\sin\theta_{\mathrm{imp}}}{\cos\theta_{\mathrm{imp}} - V_{\mathrm{T}}/V_{\mathrm{M}}}\right). \tag{8}$$

From Eq. (8), the first and second time derivative of λ_{F} can be derived as

$$\dot{\lambda}_{\mathrm{F}} = \dot{\gamma}_{\mathrm{T}} = \frac{a_{\mathrm{T}}}{V_{\mathrm{T}}}, \qquad \ddot{\lambda}_{\mathrm{F}} = \ddot{\gamma}_{\mathrm{T}} = \frac{\dot{a}_{\mathrm{T}}}{V_{\mathrm{T}}}. \tag{9}$$

The design goal of this work can be described as follows. Design a proper guidance law such that λ and $\dot{\lambda}$ could converge to λ_{F} and $\dot{\lambda}_{\mathrm{F}}$ at the time of interception.

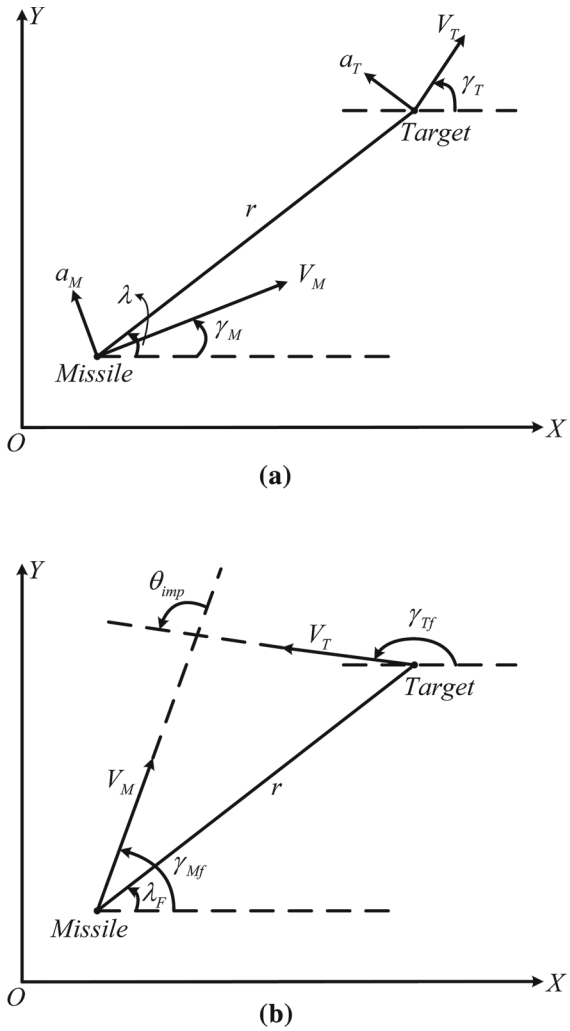

Fig. 1 Relative position of the missile and the target. **a** Engagement geometry. **b** Collision course

3 Function-based finite-time sliding mode control

In this part, the basic principle of FBFTSMC will be introduced. First, let us consider the following typical second-order nonlinear uncertain system:

$$\begin{cases} \dot{x}_1 = x_2 \\ \dot{x}_2 = g(x) + b(x)u + d \end{cases} \tag{10}$$

where $x = [x_1, x_2]^{\mathrm{T}}$ is the state vector, u is the control input, $g(x)$ and $b(x) \neq 0$ are assumed to be known functions of x, and d is the lumped uncertainty which is bounded but unknown. The design objective of this control problem is to find a controller such that the system states would converge to zero at the designated finite time t_{f}, i.e., $\lim_{t \to t_{\mathrm{f}}} x_1 \to 0$, $\lim_{t \to t_{\mathrm{f}}} x_2 \to 0$.

Before moving on, a specific variable is designed as follows:

$$\sigma = x_2 - \frac{n\dot{f}(t)}{f(t)} x_1 \tag{11}$$

where $n > 1$ is a constant and $f(t)$ is a time-varying function which satisfies: (1) $f(t)$ is second-order differentiable, (2) $f(t) \neq 0$ for $0 \leq t < t_{\mathrm{f}}$ and $f(t_{\mathrm{f}}) = 0$.

Then, the sliding surface function is designed by adding an additional term to σ:

$$s_1 = \sigma + \xi \tag{12}$$

where $\xi(0) = -\sigma(0)$, $\dot{\xi} = -\frac{m\dot{f}(t)}{f(t)}\sigma$ and $m \geq n$ is a constant. Consider the control law (13)

$$\begin{aligned} u = \frac{1}{b(x)} \Bigg[& \frac{nf(t)\ddot{f}(t) - (m+1)n(\dot{f}(t))^2}{(f(t))^2} x_1 \\ & + \frac{(m+n)\dot{f}(t)}{f(t)} x_2 - g(x) - k\mathrm{sgn}(s_1) \Bigg] \end{aligned} \tag{13}$$

where the switching gain $k > ||d||_\infty$, and one can get the following theorem.

Theorem 1 *For the nonlinear uncertain system described in Eq. (10), by adopting the sliding surface function (12) and the control law (13), a GSM is realized. Furthermore, the state variables x_1 and x_2 will both converge to zero at $t = t_{\mathrm{f}}$.*

Proof Consider the following positive Lyapunov function candidate

$$V = \frac{1}{2} s_1^2. \tag{14}$$

Taking the time derivative of V and making use of the control law (13), one gets

$$\dot{V} = s_1(-k\mathrm{sgn}(s_1) + d) \leq -(k - ||d||_\infty)|s_1| \leq 0. \tag{15}$$

Apparently, $\dot{V}$ is nonpositive, and hence $V \leq V(0)$. Further notice that $s_1(0) = \sigma(0) + \xi(0) = 0$, one gets $V \leq 0$. On the other hand, $V \geq 0$ is ensured by Eq. (14). Therefore, it is concluded that $V \equiv 0$, implying $s_1 \equiv 0$ for $t \in [0, t_{\mathrm{f}}]$. Thus, a GSM is realized.

Then, using Eq. (12), the derivative of $s_1 = 0$ can be found as

$$\dot{s}_1 = \dot{\sigma} - \frac{m\dot{f}(t)}{f(t)}\sigma = 0. \tag{16}$$

Rearranging variables, Eq. (16) can be rewritten as

$$\frac{1}{\sigma} d\sigma = \frac{m\dot{f}(t)}{f(t)} dt. \tag{17}$$

Then, by integrating Eq. (17) from $(0, \sigma(0))$ to some later point $(t, \sigma(t))$, the analytic solution for σ can be obtained as

$$\sigma = b_2 (f(t))^{\mathrm{m}} \tag{18}$$

where $b_2 = \frac{\sigma(0)}{(f(0))^m}$ is a constant.

Substituting Eq. (11) into Eq. (18), one gets

$$x_2 - \frac{n\dot{f}(t)}{f(t)} x_1 = b_2 (f(t))^{\mathrm{m}}. \tag{19}$$

The equation above is a typical first-order linear differential equation whose solution can be solved as

$$x_1 = (f(t))^n \left(b_3 + b_2 F(t) \right) \tag{20}$$

where $F(t) = \int (f(t))^{\mathrm{m-n}} \mathrm{d}t$ is the primitive function of $(f(t))^{m-n}$, and $b_3 = \frac{x_1(0)}{(f(0))^n} - b_2 F(0)$ is a constant. It is worth noticing that $F(t)$ always exists in this study because $f(t)$ is a continuous function and $m \geq n$. In addition, $F(t)$ is bounded for $t \in [0, t_f]$ because it is continuous during this time interval. Based on the above analysis and notice $f(t_{\mathrm{f}}) = 0$, it can be concluded that x_1 will converge to zero at $t = t_{\mathrm{f}}$.

Taking the time derivative of Eq. (20) yields

$$x_2 = (f(t))^{n-1}\Big[n\dot{f}(t)\big(b_3 + b_2F(t)\big) + b_2(f(t))^{m-n+1}\Big]. \tag{21}$$

From the above equation, it can be found that x_2 will also converge to zero at $t = t_\mathrm{f}$. □

Remark 1 By inspecting Eq. (13), it can be seen that $f(t)$ appears in the denominator of two terms in the control law. Since $f(t_\mathrm{f}) = 0$, it would appear to lead to a singularity at $t = t_\mathrm{f}$. As a matter of fact, the singularity can be eliminated by properly tuning the value of n. Substituting the analytic solutions of x_1 and x_2 into the control law (13) yields

$$\begin{aligned} u = \Big[&\big(nf(t)\ddot{f}(t) - (m+1)n(\dot{f}(t))^2\big)(b_3 + b_2F(t))(f(t))^{n-2} \\ &-g(x) - k\mathrm{sgn}(s_1) + (m+n)\dot{f}(t)\big(n\dot{f}(t)\big(b_3 + b_2F(t)\big) \\ &+ b_2(f(t))^{m-n+1}\big)(f(t))^{n-2}\Big]\frac{1}{b(x)}. \end{aligned} \tag{22}$$

From the above equation, it can be concluded that the singular problem is avoided as long as $n \geq 2$. Therefore, the value of n should be chosen no less than two during the implementation of the control law.

Remark 2 If there is control saturation during the implementation of the control law (13), the system states would deviate from the sliding surface (12) and thus the control performance would be affected. However, if the sliding surface can be reached at some finite time before t_f, e.g., $s_1 = 0$ for $t_\mathrm{r} \leq t \leq t_\mathrm{f}$, the system states can still be driven to zero at $t = t_\mathrm{f}$. This is because from t_r onward, the system states x_1 and x_2 are still governed by Eqs. (20) and (21) with the constants $b_2 = \frac{\sigma(t_\mathrm{r})}{(f(t_\mathrm{r}))^m}$ and $b_3 = \frac{x_1(t_\mathrm{r})}{(f(t_\mathrm{r}))^n} - b_2F(t_\mathrm{r})$.

Remark 3 Note that although the proposed controller guarantees fixed time convergence, the control action is over at the desired final time t_f. Therefore, the developed control method is suitable for the practical control problems which require a goal to be achieved in a given time.

Remark 4 The SMC approach proposed in this work is closely related to the time-varying function $f(t)$. Besides, such a controller can guarantee finite-time convergence of the system states. In this sense, the proposed method is named as FBFTSMC algorithm. To derive a feasible impact angle control law, a simple expression for $f(t)$ is selected, which takes the form of

$$f(t) = t_\mathrm{f} - t. \tag{23}$$

It can be easily verified that Eq. (23) meets all the requirements for $f(t)$. Since the expression for $f(t)$ is not unique, it gives lots of flexibility in the associated guidance law design. For example, $f(t)$ can be specially designed to provide additional degrees of freedom for other control goals. This characteristic would be further analyzed in Sect. 5.4.

4 Impact angle constrained guidance law

This section details the steps in the application of the FBFTSMC algorithm to the impact angle constrained guidance problem. Note that the stationary and constant-velocity target scenarios can be treated as special cases of the maneuvering target scenario. The guidance laws in this part are developed for the general case of a maneuvering target. Before moving on, the following assumption is made as in [17–19]; that is, only the target acceleration is unknown and other parameters are assumed known.

By differentiating Eq. (2), one gets

$$\ddot{\lambda} = -\frac{2\dot{r}\dot{\lambda}}{r} + \frac{\cos(\gamma_\mathrm{T} - \lambda)}{r}a_\mathrm{T} - \frac{\cos(\gamma_\mathrm{M} - \lambda)}{r}a_\mathrm{M} \tag{24}$$

which exhibits the relationship between the LOS angle λ and the missile acceleration a_M. Note, from Eq. (24), that λ can be controlled only when $|\gamma_\mathrm{M} - \lambda| \neq \pi/2$. As has been shown in [17,18], $|\gamma_\mathrm{M} - \lambda| = \pi/2$ is an unstable equilibrium point due to $\dot{\gamma}_\mathrm{M} - \dot{\lambda} \neq 0$ when $|\gamma_\mathrm{M} - \lambda| = \pi/2$. Hence, a_M can be employed to control λ.

4.1 Guidance law design

In this subsection, the guidance law is developed for a maneuvering target, whose acceleration and flight path angle vary with time. The LOS angle error Λ is expressed as

$$\Lambda = \lambda - \lambda_\mathrm{F}. \tag{25}$$

Note, from Eq. (9), that λ_F and $\dot{\lambda}_\mathrm{F}$ vary with time. Hence, the first and second time derivatives of the LOS angle error can be obtained as

$$\begin{cases} \dot{\Lambda} = \dot{\lambda} - \frac{a_T}{V_T} \\ \ddot{\Lambda} = -\frac{2\dot{r}\dot{\lambda}}{r} + \frac{\cos(\gamma_T-\lambda)}{r}a_T - \frac{\cos(\gamma_M-\lambda)}{r}a_M - \frac{\dot{a}_T}{V_T}. \end{cases} \tag{26}$$

Apparently, Eq. (26) is a nonlinear second-order system.

According to Eqs. (11), (12) and (23), the sliding surface is designed as

$$S_1 = \dot{\Lambda} + \frac{n\Lambda}{t_f - t} + \xi_1 \tag{27}$$

where $\xi_1(0) = -\dot{\Lambda}(0) - \frac{n\Lambda(0)}{t_f}$ and $\dot{\xi}_1 = \frac{m}{t_f - t}\left(\dot{\Lambda} + \frac{n\Lambda}{t_f - t}\right)$.

Remark 5 From Eq. (27), it can be seen that the term $t_f - t$ is involved in the design of the associated sliding surface. The final flight time t_f, however, cannot be easily known in advance, and hence, it cannot be specified here. To solve this problem, Eq. (27) is rewritten as

$$S_1 = \dot{\Lambda} + \frac{n\Lambda}{t_{go}} + \xi_1 \tag{28}$$

where $t_{go} = \frac{r}{V_c}$. $V_c = -\dot{r}$ denotes the closing velocity between the missile and the target. Correspondingly, the variable ξ_1 satisfies $\xi_1(0) = -\dot{\Lambda}(0) - \frac{n\Lambda(0)}{t_{go}(0)}$ and $\dot{\xi}_1 = \frac{m}{t_{go}}\left(\dot{\Lambda} + \frac{n\Lambda}{t_{go}}\right)$.

Assume the target acceleration a_T is known and treat the term $\frac{\dot{a}_T}{V_T}$ as the disturbance, the associated guidance command can be derived by using the FBFTSMC algorithm, which takes the form of

$$\begin{aligned} a_M = \frac{r}{\cos(\gamma_M - \lambda)}\Bigg[& \frac{(m+n)\left(\dot{\lambda} - \frac{a_T}{V_T}\right)}{t_{go}} \\ & + \frac{(m+1)n(\lambda - \lambda_F)}{t_{go}^2} - \frac{2\dot{r}\dot{\lambda}}{r} \\ & + \frac{\cos(\gamma_T - \lambda)}{r}a_T + k_1 \mathrm{sgn}(S_1)\Bigg] \end{aligned} \tag{29}$$

where $k_1 > ||\frac{\dot{a}_T}{V_T}||_\infty$.

Remark 6 For the case of intercepting a stationary or constant-velocity target, one gets $a_T = 0$. Therefore, the guidance law (29) can be simplified to the following form

$$\begin{aligned} a_M = \frac{r}{\cos(\gamma_M - \lambda)}\Bigg[& \frac{(m+n)\dot{\lambda}}{t_{go}} \\ & + \frac{(m+1)n(\lambda - \lambda_F)}{t_{go}^2} - \frac{2\dot{r}\dot{\lambda}}{r} + k_1 \mathrm{sgn}(S_1)\Bigg] \end{aligned} \tag{30}$$

It is interesting to note that the continuous counterpart in Eq. (30) can be further rewritten as $\frac{1}{\cos(\gamma_M - \lambda)}\left[(m+n+2)V_c\dot{\lambda} + \frac{(m+1)n}{t_{go}}V_c(\lambda - \lambda_F)\right]$, which is similar to the so-called biased PNG with an additional term in the denominator. The first component controls the missile to hit the target, and the second component contributes to the achievement of the desired LOS angle. Because the LOS angle error and angular rate would both be driven to zero at the time of interception, zero magnitude of the guidance command can be achieved.

It can be seen from Eqs. (26), (28) and (29) that the target acceleration really plays an important role in the guidance law development. In practical implementation, however, it is usually difficult to measure the target acceleration directly. A possible solution to this problem is using the current system states to estimate the target acceleration. Motivated by the work in [19], the LESO is employed to obtain the estimation of a_T. First, we define a new variable $V_\lambda = r\dot{\lambda}$, which corresponds to the relative velocity perpendicular to the LOS. Differentiating V_λ with respect to t yields

$$\dot{V}_\lambda = -\dot{r}\dot{\lambda} + a_T\cos(\gamma_T - \lambda) - a_M\cos(\gamma_M - \lambda). \tag{31}$$

Taking $a_{T\lambda} = a_T\cos(\gamma_T - \lambda)$ as an augmented state, one can get the following second-order dynamic system

$$\begin{cases} \dot{V}_\lambda = -\dot{r}\dot{\lambda} + a_{T\lambda} - a_M\cos(\gamma_M - \lambda) \\ \dot{a}_{T\lambda} = l. \end{cases} \tag{32}$$

Then, the second-order LESO for the aforementioned system can be designed as [19]

$$\begin{cases} \dot{z}_1 = z_2 - \zeta_1 e_1 - \dot{r}\dot{\lambda} - a_M\cos(\gamma_M - \lambda) \\ \dot{z}_2 = -\zeta_2 e_1 \end{cases} \tag{33}$$

where $e_1 = z_1 - V_\lambda$, $e_2 = z_2 - a_{T\lambda}$, $\zeta_1 = 2\omega_0$, $\zeta_2 = \omega_0^2$ and ω_0 is the bandwidth of the observer. Assume the initial values of V_λ and $a_{T\lambda}$ are $V_{\lambda 0}$ and $a_{T\lambda 0}$, respectively. In practice, however, $a_{T\lambda 0}$ is hard to obtain. So the initial values of z_1 and z_2 are set to $V_{\lambda 0}$ and 0, respectively.

The convergence of the LESO can be established by the following lemma.

Lemma 1 *[28] Assuming l is bounded, there exist a constant p_i and a finite time $t_p > 0$ such that $|e_i(t)| \leq$*

p_i, $i = 1, 2$, $\forall t \geq t_p > 0$ *and* $\omega_0 > 0$. *Furthermore,* $p_i = O\left(\frac{1}{\omega_0^q}\right)$, *for some positive integer* q.

From Eq. (32), it can be easily found that l is bounded. Therefore, via tuning ω_0 appropriately, the observer output z_1 and z_2 would both converge into a close neighborhood of the actual states V_λ and $a_{\mathrm{T}\lambda}$ in finite time. Then, the target acceleration can be obtained as

$$a_{\mathrm{T}} = \frac{a_{\mathrm{T}\lambda}}{\cos(\gamma_{\mathrm{T}} - \lambda)} = \frac{z_2}{\cos(\gamma_{\mathrm{T}} - \lambda)}. \tag{34}$$

Substituting Eq. (34) into Eqs. (28) and (29), the modified sliding surface and guidance command can be derived as

$$S_{1m} = \dot{\lambda} - \frac{z_2}{V_{\mathrm{T}}\cos(\gamma_{\mathrm{T}} - \lambda)} + \frac{n(\lambda - \lambda_{\mathrm{F}})}{t_{\mathrm{go}}} + \xi_{1m}, \tag{35}$$

$$a_{\mathrm{Mm}} = \frac{r}{\cos(\gamma_{\mathrm{M}} - \lambda)}\left[\frac{(m+n)\left(\dot{\lambda} - \frac{z_2}{V_{\mathrm{T}}\cos(\gamma_{\mathrm{T}} - \lambda)}\right)}{t_{\mathrm{go}}} - \frac{2\dot{r}\dot{\lambda}}{r} + \frac{(m+1)n(\lambda - \lambda_{\mathrm{F}})}{t_{\mathrm{go}}^2} + \frac{z_2}{r} + k_{1m}\mathrm{sgn}(S_{1m})\right], \tag{36}$$

where $\xi_{1m}(0) = -\dot{\lambda}(0) - \frac{n(\lambda(0) - \lambda_F(0))}{t_{\mathrm{go}}(0)}$, $\dot{\xi}_{1m} = \frac{m}{t_{\mathrm{go}}}\left(\dot{\lambda} - \frac{z_2}{V_{\mathrm{T}}\cos(\gamma_{\mathrm{T}} - \lambda)} + \frac{n(\lambda - \lambda_{\mathrm{F}})}{t_{\mathrm{go}}}\right)$ and k_{1m} corresponds to the switching gain which satisfies

$$k_{1m} > \left\| \frac{\cos(\gamma_{\mathrm{T}} - \lambda)a_{\mathrm{T}} - z_2}{r} \right\|_\infty + \frac{\|W(t)\|_\infty}{V_{\mathrm{T}}} + \left\| \frac{n}{t_{\mathrm{go}}}\left(\frac{z_2}{V_{\mathrm{T}}\cos(\gamma_{\mathrm{T}} - \lambda)} - \frac{a_{\mathrm{T}}}{V_{\mathrm{T}}}\right) \right\|_\infty + \left\| \frac{\dot{a}_{\mathrm{T}}}{V_{\mathrm{T}}} \right\|_\infty \tag{37}$$

where $W(t) = \frac{d}{dt}\left(\frac{z_2}{\cos(\gamma_{\mathrm{T}} - \lambda)}\right)$.

Theorem 2 *With the sliding mode manifold given by Eq. (35), observer obtained by Eq. (33), the trajectory of the closed-loop system (26) can be driven into a neighborhood of the sliding surface (28) in finite time with the guidance law (36).*

Proof Consider the Lyapunov candidate $V_1 = 0.5S_{1m}^2$. Taking the derivative of V_1 and making use of the guidance law (36) yield $\dot{V}_1 \leq 0$. Therefore, it can be concluded that $V_1 \leq V_1(0)$. Note that $S_{1m}(0) = 0$, one gets $V_1 \leq 0$. Further considering $V_1 \geq 0$, it can be concluded that $V_1 \equiv 0$, which implies $S_{1m} \equiv 0$. From Lemma 1, the observer errors e_1 and e_2 can converge to a small vicinity of zero in finite time by tuning ω_0 properly. Therefore, the system states can be ensured to reach a close neighborhood of the sliding surface (28) in finite time. □

Remark 7 From the above theorem, it can be concluded that although S_{1m} is treated as the sliding surface, the closed-loop system (26) can be driven into a close neighborhood of $S_1 = 0$ in finite time. Since the size of the observer error can be controlled by the user, the difference between $S_{1m} = 0$ and $S_1 = 0$ can be reduced to a negligible magnitude. Associating this result with the FBFTSMC algorithm, we can conclude that the LOS angle λ and its derivative $\dot{\lambda}$ will converge to λ_F and $\dot{\lambda}_F$, respectively, at the time of interception.

As an inherent problem of SMC, chattering is an undesired phenomenon because it involves high control action that may excite high-frequency unmodeled dynamics. To soften chattering, the saturation function $\mathrm{sat}(S)$ is used to replace the sign function $\mathrm{sgn}(S)$ in the implementation of the proposed laws, which takes the form of

$$\mathrm{sat}(S) = \begin{cases} \varepsilon^{-1}S, & |S| \leq \varepsilon \\ \mathrm{sgn}(S), & \text{otherwise} \end{cases} \tag{38}$$

where ε is the boundary layer thickness.

4.2 Guidance logic for all-aspect interception

To achieve all-aspect interception, the guidance law is required to ensure interception for all states of the missile and the target during the homing engagement. To this end, an SMC-based approach is investigated in [27]. In this work, two different sliding surfaces are designed and a specific switching logic is developed to make the guidance laws to switch between enforcing sliding mode on one of these two surfaces. Because two kinds of guidance laws are designed, two sets of guidance parameters are required, which adds difficulties to the implementation of this method. More importantly, if the guidance parameters are not properly tuned, the sliding mode may not be enforced from the first sliding surface to the second sliding surface, and thus, the result would be a miss.

From the basics of terminal guidance, it is known that the closing velocity V_{c} should be larger than 0 to guarantee a successful interception. But in the large initial heading error cases, V_{c} may have a negative value

at the early stage, which would give rise to an unacceptable t_{go} estimation (i.e., $t_{go} < 0$). To solve this problem, the time-to-go estimation is modified to the following form:

$$t_{go} = \begin{cases} r/V_c, & V_c > 0 \\ 2r/V_M, & V_c \le 0 \end{cases} \tag{39}$$

It should be noted that although the estimation of t_{go} will always have a positive value with this modification, the estimated value may be quite different from its true value, and thus, the performance of the proposed guidance law may also deteriorate in large initial heading error cases. Although some modified methods have been presented to improve the precision of t_{go} estimation [25,26], the stationary target scenario is assumed. So these methods may not produce accurate t_{go} estimates in the presence of a moving target.

From the above analysis, it can be found that the closing velocity V_c may be negative when the heading error is really large, and thus, the proposed guidance law cannot ensure successful interception. To achieve all-aspect interception, the closing velocity should always be positive before the time of interception. Motivated by this conclusion, a suitable guidance logic is developed to realize all-aspect interception, which takes the form of

$$a_M = \begin{cases} a_{M\max}\mathrm{sgn}(a_{M0}), & \text{if } V_c \le \kappa \\ a_M, & \text{if } V_c > \kappa \end{cases} \tag{40}$$

where $a_{M\max} > 0$ is the maximum lateral acceleration that the missile can generate, a_{M0} represents the initial value of a_M and κ is a positive constant that needs to be determined. For the case of intercepting a nonmaneuvering target, κ can be set to a small value, e.g., 0. For the case of intercepting a maneuvering target, a relatively large value of κ is required. This guidance logic can be explained as follows. First, by using the maximum lateral acceleration, the missile changes its course quickly so that the large heading error can be reduced to a relatively small magnitude (i.e., $V_c > \kappa$ is achieved). Then, the proposed guidance law can be used during the remaining flight to realize a desired interception course. It should be noted that if $V_c > \kappa$ maintains for the entire homing phase, only the proposed guidance law would be used. Because the proposed guidance logic possesses a simple format and requires no additional switching surfaces, it is more practical than the method in [27].

Table 1 Simulation parameters

Parameters	Values	Parameters	Values
V_M	500 m/s	ε (for Cases 1, 2)	0.1
γ_{M0}	30°	ε (for Cases 3, 4)	0.8
V_T	250 m/s	$k_{1\,m}$ (for Cases 1, 2)	0.01
γ_{T0}	120°	$k_{1\,m}$ (for Cases 3, 4)	0.05
n	2	κ (for Cases 1, 2)	0 m/s
m	2	κ (for Cases 3, 4)	300 m/s
ω_0	100		

5 Numerical simulations

To validate the effectiveness of the proposed guidance laws, simulations for a variety of scenarios are performed in this section. To begin with, the initial conditions of the missile–target engagement are illustrated. The initial LOS angle and the distance between the missile and the target are assumed to be 30° and 10 km, respectively. The initial position of missile in inertial coordinate system is assumed to be $X_{M0} = Y_{M0} = 0$ m. To evaluate the performance of the proposed guidance laws in the presence of system lag, the simulation studies in this section are all performed with a first-order lag system for which the time constant is 0.1 s. The maximum lateral acceleration $a_{M\max}$ is set to 400 m/s^2, as used in [18]. Other initial conditions as well as the guidance parameters used in the following cases, unless specified, are listed in Table 1. All the simulations are terminated at a closing distance of less than 0.1 m.

5.1 Case 1: stationary target

In the first study of this case, the proposed guidance law is implemented to intercept a stationary target from different directions and the desired impact angles are chosen as 0°, 90°, 180° and −90°. The associated results are presented in Fig. 2.

From Fig. 2a, it can be seen that the proposed guidance law is able to steer the missile to the collision course and the desired impact angles are achieved at the time of interception. It can be seen from Fig. 2b that a relatively large magnitude of lateral acceleration is required during the period when the missile changes its course. Once the desired LOS angle is achieved, there is no need for the missile to change its course any more. Therefore, the lateral acceleration converges

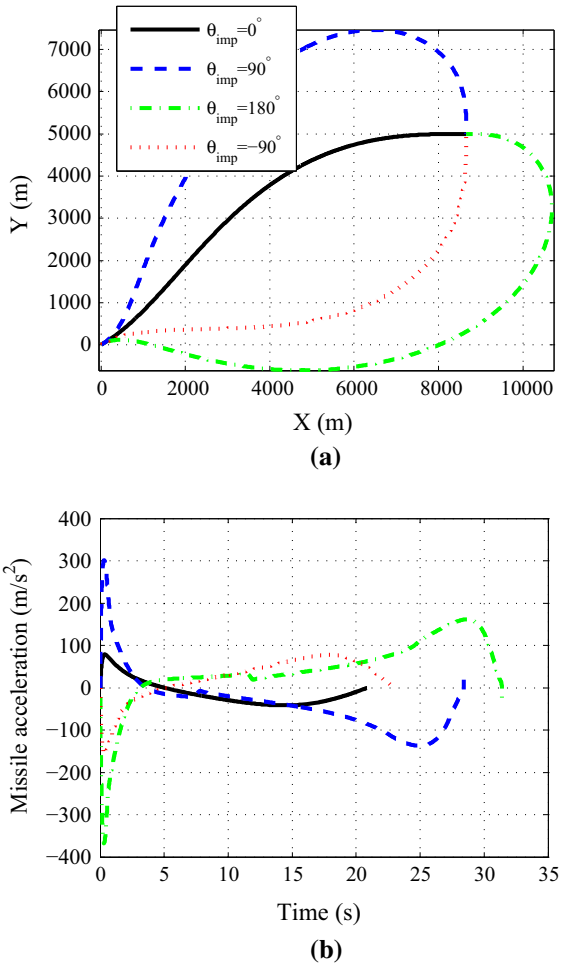

Fig. 2 Interception of a stationary target at different impact angles. **a** Trajectories of the missile. **b** Missile acceleration histories

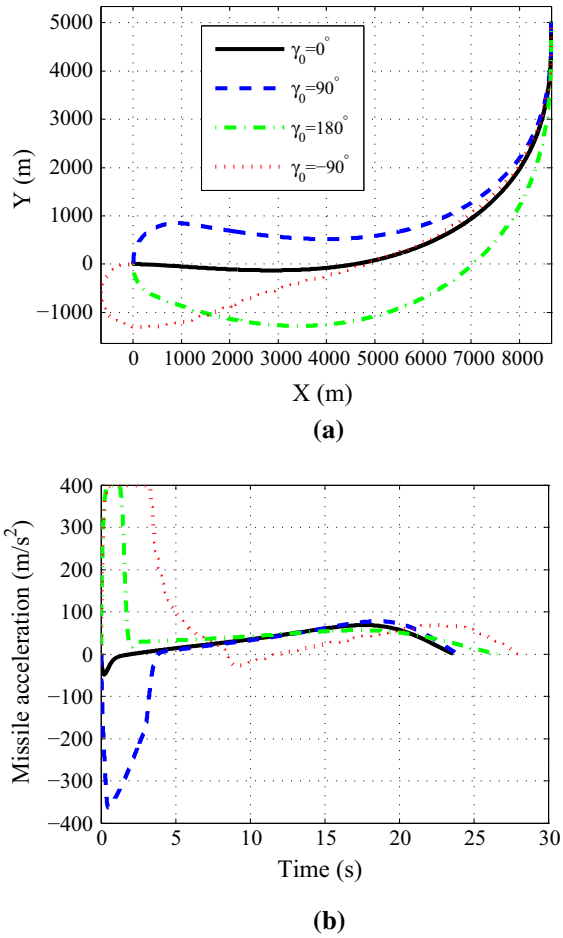

Fig. 3 Interception of a stationary target at a given impact angle but with different initial flight path angles. **a** Trajectories of the missile. **b** Missile acceleration histories

to zero at the time of interception. Besides, it can be found that no sudden change occurs in the associated guidance command histories due to the GSM nature of FBFTSMC.

The next simulation is performed with different launch angles of 0°, 90°, 180° and −90° and a specific impact angle of −90°, with the results shown in Fig. 3.

As can be seen from Fig. 3a, the missile can be steered to the same interception course decided by the desired LOS angle. For the cases of $\gamma_0 = 180°$ and $\gamma_0 = -90°$, the initial heading errors are very large. According to the guidance logic (40), the maximum lateral acceleration, as seen in Fig. 3b, is imposed during the initial period in these cases. When the heading errors are reduced to a relatively small magnitude, which in this case is $V_c > 0$, the proposed law is then employed to achieve successful interceptions. It should be noted that the all-aspect capability of the guidance law against a stationary target is justified by the results in this subsection.

5.2 Case 2: constant-velocity target

In this part, the case of intercepting a constant-velocity target in three kinds of engagement geometries, i.e., tail-chase, lateral-impact and head-on, is first considered. In this regard, the desired impact angles are selected as 0°, 90° and 180°, respectively. Since the target does not execute a maneuver, its flight path angle maintains a constant value of 120°. The results for this set of simulations are shown in Fig. 4.

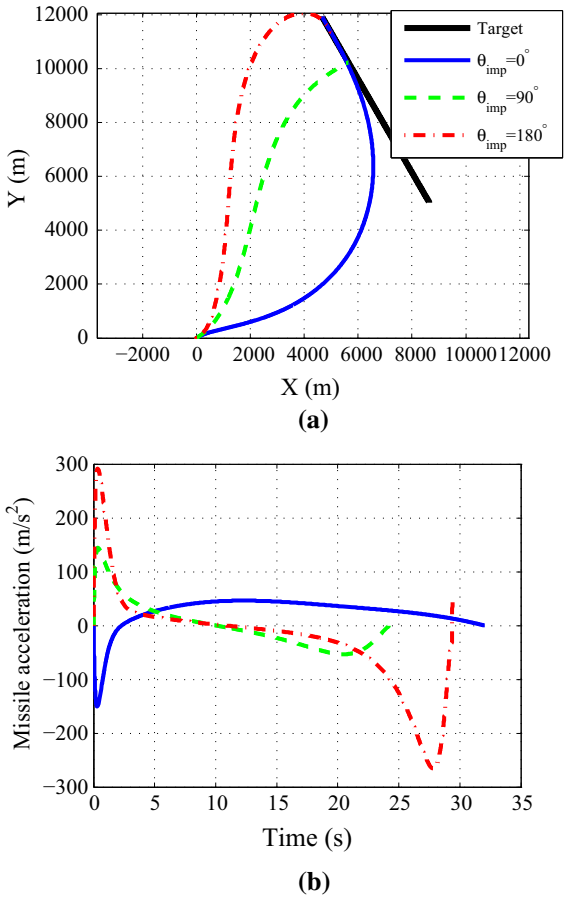

Fig. 4 Interception of a constant-velocity target at different impact angles. **a** Trajectories of missile and target. **b** Missile acceleration histories

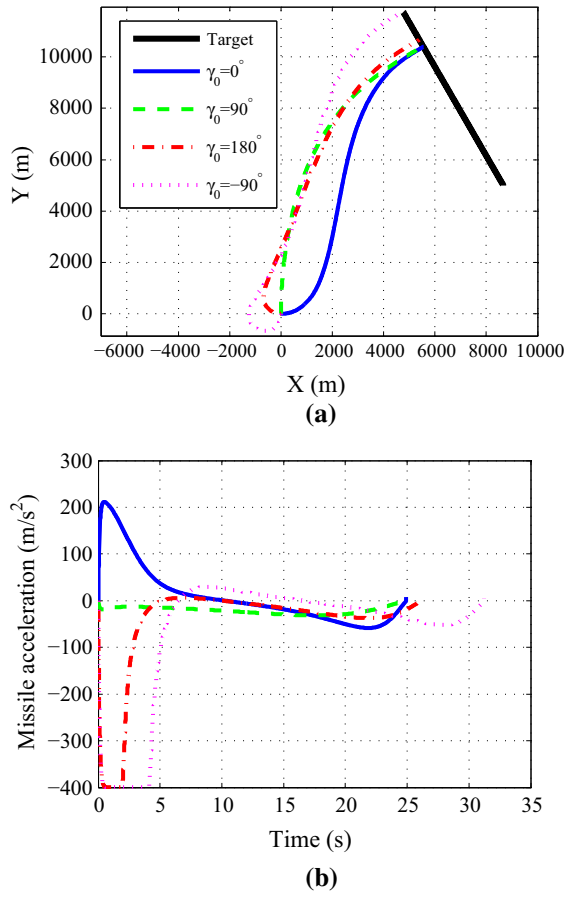

Fig. 5 Interception of a constant-velocity target at a given impact angle but with different initial flight path angles. **a** Trajectories of missile and target. **b** Missile acceleration histories

For each specified interception geometry, Fig. 4a shows that the proposed guidance law generates a feasible homing trajectory which fulfills the impact angle constraint. The average impact angle error for the three cases is 0.0784°. As shown in Fig. 4b, the lateral accelerations must initially increase to force the missile into the desired engagement dynamics that are governed by the sliding surfaces. Furthermore, high control effort is applied during the period when the missile performs a turning back maneuver.

The next set of simulations in this part involves engaging a constant-velocity target at a desired impact angle of 90° but for different initial launch angles. The associated results are represented in Fig. 5. By inspecting these results, similar conclusions to the stationary target case can be drawn. Also, these results demonstrate the all-aspect capability of the guidance law against a constant-velocity target.

5.3 Case 3: constant maneuvering target

In this part, the simulations are performed for the scenario of intercepting a maneuvering target at a desired impact angle of 90° but for different initial flight path angles. The target maneuver is assumed to be $a_T = 20\,\mathrm{m/s^2}$.

The results for this case are presented in Fig. 6. For simplicity of notation, "True value" and "Estimated value" are replaced by "TV" and "EV" in illustration. From Fig. 6a, it can be seen that the proposed guidance logic can control the missile to the desired interception course even in the presence of large initial heading errors and a high maneuvering target. The estimation of the unknown target acceleration, as shown in Fig. 6b, converges to $19.5\,\mathrm{m/s^2}$ in about 0.8 s and then stays in the interval of 19.9 and $20.1\,\mathrm{m/s^2}$, which implies high estimating precision of the target acceleration by

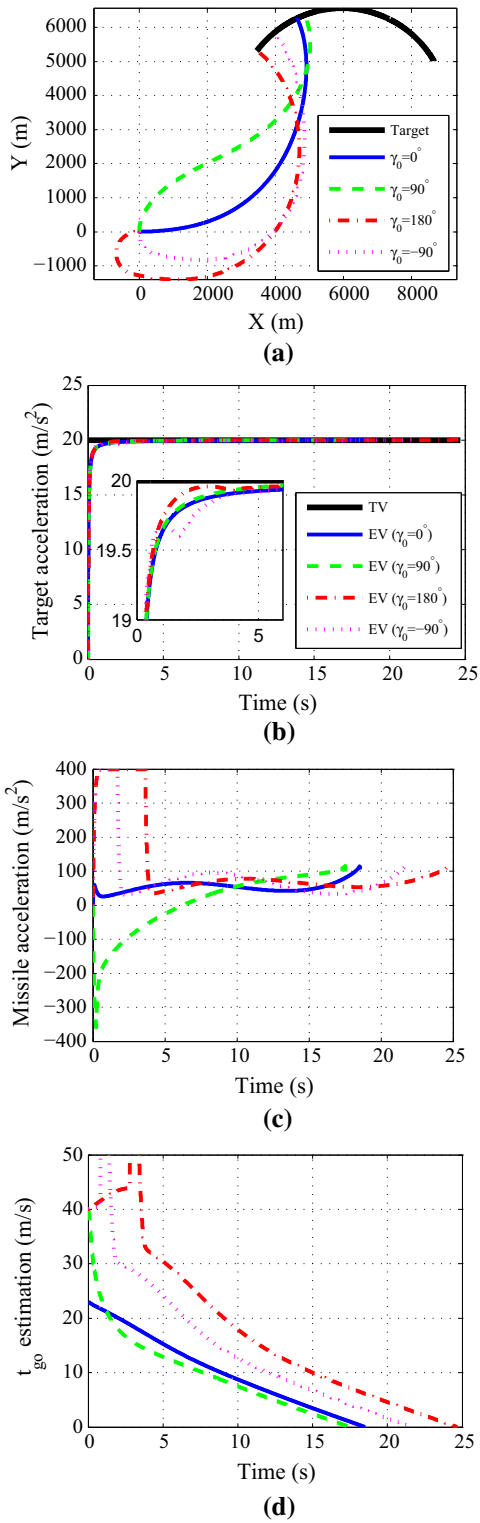

Fig. 6 Results for intercepting a constant maneuvering target. **a** Trajectories of missile and target. **b** Estimation of target acceleration. **c** Missile acceleration histories. **d** t_{go} Estimation

the LESO. Figure 6c shows that the maximum lateral acceleration is applied for the cases of $\gamma_0 = 180°$ and $\gamma_0 = -90°$ at the early stage due to large initial heading errors. When the heading error is reduced to a relatively small magnitude, the term $\frac{r}{V_c}$ is able to provide good estimates of t_{go} for the implementation of the guidance law (see Fig. 6d).

5.4 Case 4: results with different $f(t)$

In the derivation of guidance law (36), $f(t)$ is chosen as the time to go. As mentioned in Remark 4, the selection of $f(t)$ is not unique and it gives lots of flexibility in the guidance law design. In order to verify this characteristic, the results with different $f(t)$ are analyzed in this subsection. According to the constraints for $f(t)$, the time-varying function can be chosen as polynomial functions of the time to go. Without loss of generality, $f(t)$ is selected as

$$f(t) = At_{go}^2 + t_{go} \tag{41}$$

Then, the corresponding sliding surface and guidance command can be derived as

$$S_2 = \dot{\lambda} - \frac{z_2}{V_T \cos(\gamma_T - \lambda)} + \frac{n(2At_{go}+1)}{At_{go}^2 + t_{go}}(\lambda - \lambda_F) + \xi_2 \tag{42}$$

$$\begin{aligned} a_M = -\frac{r}{\cos(\gamma_M - \lambda)} \Bigg[& \frac{2\dot{r}\dot{\lambda}}{r} - \frac{z_2}{r} - k_2 \mathrm{sgn}(S_2) \\ & - \frac{(m+n)(2At_{go}+1)}{At_{go}^2 + t_{go}} \left(\dot{\lambda} - \frac{z_2}{V_T \cos(\gamma_T - \lambda)} \right) \\ & \frac{2nA(At_{go}^2 + t_{go}) - (m+1)n(2At_{go}+1)^2}{(At_{go}^2 + t_{go})^2}(\lambda - \lambda_F) \Bigg] \end{aligned} \tag{43}$$

where $\xi_2(0) = -\dot{\lambda}(0) - \frac{n(2At_{go}(0)+1)}{At_{go}(0)^2 + t_{go}(0)}(\lambda(0) - \lambda_F(0))$, $\dot{\xi}_2 = \frac{m(2At_{go}+1)}{At_{go}^2+t_{go}}\left(\dot{\lambda} - \frac{z_2}{V_T \cos(\gamma_T - \lambda)} + \frac{n(2At_{go}+1)}{At_{go}^2+t_{go}}(\lambda - \lambda_F)\right)$, $k_2 > \left\| \frac{n(2At_{go}+1)}{At_{go}^2+t_{go}} \left(\frac{z_2}{V_T \cos(\gamma_T - \lambda)} - \frac{a_T}{V_T} \right) \right\|_\infty + \frac{\|W(t)\|_\infty}{V_T} + \left\| \frac{\cos(\gamma_T - \lambda)a_T - z_2}{r} \right\|_\infty + \left\| \frac{\dot{a}_T}{V_T} \right\|_\infty$. As can be seen, if we choose $A = 0$, the guidance law (43) turns out to be the guidance law (36).

In this case, the initial flight path angle is selected as 30° and other engagement conditions are the same as the simulation conditions in Sect. 5.3. Since the coefficient A can be an arbitrary constant, it is set to 0, 0.05, 0.1 and 1, respectively. The associated results are

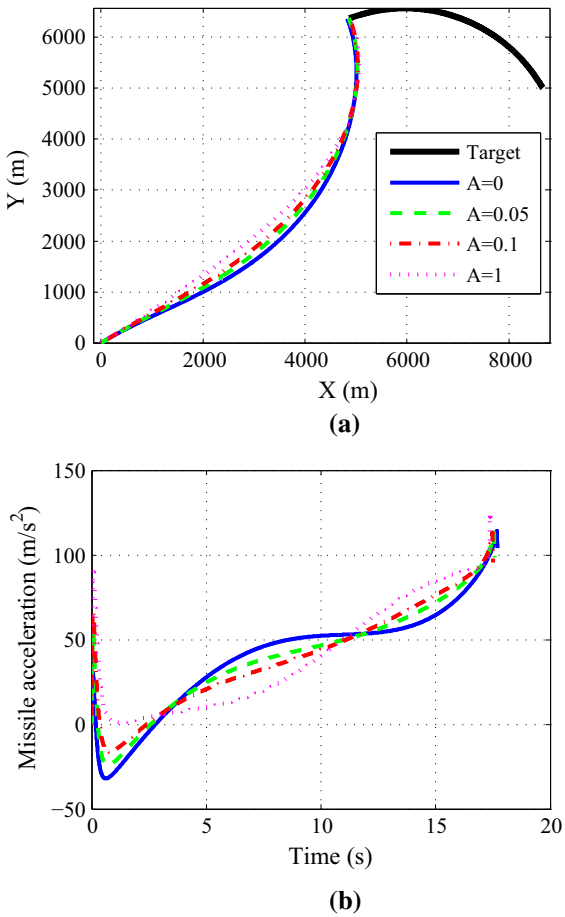

Fig. 7 Results with different $f(t)$. **a** Trajectories of missile and target. **b** Missile acceleration histories

depicted in Fig. 7. From these results, it can be concluded that the function $f(t) = At_{go}^2 + t_{go}$ can also lead to feasible homing results. In addition, the guidance performance can be adjusted by tuning the value of A. As the coefficient A increases, the guidance command during the initial phase decreases.

5.5 Case 5: comparison with NTSMC-based laws in the weaving target scenario

For comparative analysis, the guidance laws proposed in [18] and [19], which are also based on the basic principle of SMC, are carried out in this subsection. The simulations are performed for a weaving target with $a_T = 15\sin(\pi t/10)$ m/s^2. The initial flight path angle of the missile and the desired impact angle are both set to 90°. The results for this set of simulations are represented in Fig. 8.

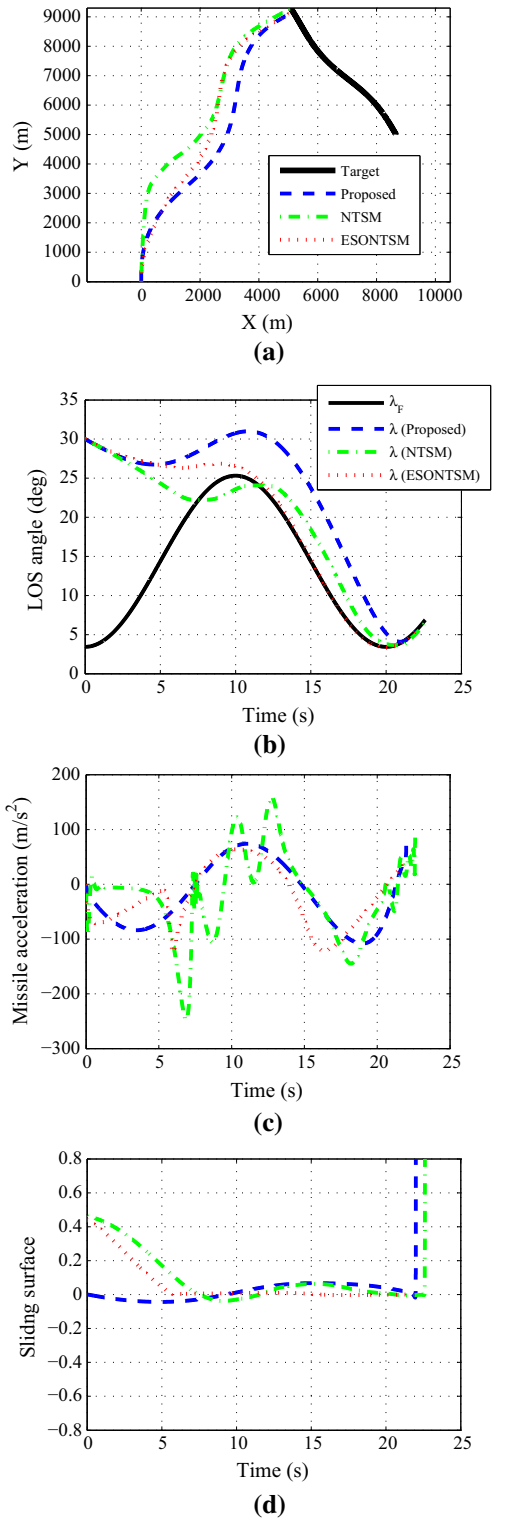

Fig. 8 Comparative analysis. **a** Trajectories of missile and target. **b** LOS angle histories. **c** Missile acceleration histories. **d** Sliding surface histories

From Fig. 8a, it can be seen that all the three guidance laws are able to guarantee successful interception. The associated impact angles are 89.9839°, 90.4829° and 90.0356°, respectively. The proposed law generates a deviation of −0.0161° compared with the desired impact angle, while the corresponding results under the NTSM [18] and the ESONTSM [19] are 0.4829° and 0.0356°, respectively. Figure 8b shows that the three guidance laws generate different LOS angle histories. Compared with the NTSMC law, the guidance law of [19] makes the LOS angle to approach its desired profile more rapidly. This is because the unknown target acceleration a_T, which is crucial for implementing the guidance laws, is estimated by the observer in [19]. The guidance law of [18], however, simply treats a_T as zero. Different from the laws in [18] and [19], the proposed guidance law would not enforce a desired LOS angle until the final time due to the inherent nature of FBFTSMC.

Figure 8c, d shows the results for the missile acceleration and the sliding surface, respectively. From Fig. 8d, it can be seen that the reaching phase is eliminated in the proposed sliding mode design compared with the work in [18] and [19]. Such a design is beneficial in terms of reducing the switching gain. As seen in Table 1, the switching gain used in this case is 0.05, while in [18] and [19], the corresponding values are chosen as 3000 and 120, respectively. Due to high switching gain and a lack of target acceleration information, the missile acceleration, under the NTSM guidance law, varies faster and experiences a higher magnitude than the other two laws. Although a modified switching gain has been presented in [19] (see Eq. (39) in [19]), the guidance command would be discontinuous (see the sudden change in the guidance law at roughly 6 s). Compared with the laws in [18] and [19], the proposed guidance law shows superior performance in the sense that more accurate impact angle can be achieved with smoother missile acceleration.

6 Conclusion

In this paper, a novel finite-time SMC method is developed, and through a challenging impact angle control guidance problem, the potential of the developed method is demonstrated. The simulation results have shown that the proposed guidance scheme is able to intercept stationary, constant-velocity and maneuvering targets from any specified direction, even in the presence of system lag and large heading errors. Also, the comparison results have demonstrated that the proposed guidance law outperforms the NTSM-based guidance laws in the sense that more accurate impact angle can be achieved with smoother missile acceleration. Future work in this area could focus on involving the impact time constraint in the guidance law design. The flexibility in the controller design can be further analyzed, which seems to have a lot of potential in solving practical finite-time control problems.

Acknowledgments This study was co-supported by National Nature Science Foundation of China (Nos. 11402020, 51407011).

References

1. Zarchan, P.: Tactical and Strategic Missile Guidance, 4th edn. AIAA Inc., New York (2002)
2. Jung, B., Kim, Y.: Guidance laws for anti-ship missiles using impact angle and impact time. In: Proceedings of the AIAA Guidance, Navigation, and Control Conference and Exhibit, Keystone, Colorado, pp. 3048–3060. Aug. (2006)
3. Kim, B.S., Lee, J.G., Han, H.S.: Biased PNG law for impact with angular constraint. IEEE Trans. Aerosp. Electron. Syst. **34**(1), 277–288 (1998)
4. Ratnoo, A., Ghose, D.: Impact angle constrained interception of stationary targets. J. Guid. Control Dyn. **31**(6), 1816–1821 (2008)
5. Ratnoo, A., Ghose, D.: Impact angle constrained guidance against nonstationary nonmaneuvering targets. J. Guid. Control Dyn. **33**(1), 269–275 (2010)
6. Ghosh, S., Ghose, D., Raha, S.: Three dimensional retro-PN based impact time control for higher speed nonmaneuvering targets. In: Proceedings of the IEEE 52nd Annual Conference on Decision and Control, Firenze, Italy, pp. 4865–4870 (2013)
7. Yu, W., Chen, W.: Guidance law with circular no-fly zone constraint. Nonlinear Dyn. **78**(3), 1953–1971 (2014)
8. Ming, X., Balakrishnan, S.N., Ohlmeyer, E.J.: Integrated guidance and control of missiles with θ-D method. IEEE Trans. Control Syst. Technol. **14**(6), 981–992 (2006)
9. Moosapour, S.H., Bagherzadeh, M., Alizadeh, G., et al.: Backstepping guidance law design for missile against maneuvering targets. In: Proceedings of 2nd International Conference on Control, Instrumentation and Automation, ICCIA, pp. 600–605 (2011)
10. Yanushevvsky, R.T.: Concerning Lyapunov-based guidance. J. Guid. Control Dyn. **29**(2), 509–511 (2006)
11. Bhat, S.P., Bernstein, D.S.: Finite-time stability of homogeneous systems. In: Proceedings of the American Control Conference, Albuquerque, New Mexico, pp. 2513–2514. June (1997)
12. Zhou, D., Sun, S., Teo, K.L.: Guidance laws with finite time convergence. J. Guid. Control Dyn. **32**(6), 1838–1846 (2009)

13. Sun, S., Zhou, D., Hou, W.T.: A guidance law with finite time convergence accounting for autopilot lag. Aerosp. Sci. Technol. **25**(1), 132–137 (2013)
14. Zhao, Y., Sheng, Y.Z., Liu, X.D.: Sliding mode control based guidance law with impact angle constraint. Chin. J. Aeronaut. **27**(1), 145–152 (2014)
15. Zhang, Y., Sun, M., Chen, Z.: Finite-time convergent guidance law with impact angle constraint based on sliding-mode control. Nonlinear Dyn. **70**(1), 619–625 (2012)
16. He, S., Lin, D., Wang, J.: Robust terminal angle constraint guidance law with autopilot lag for intercepting maneuvering targets. Nonlinear Dyn. **81**(1), 881–892 (2015)
17. Kumar, S.R., Rao, S., Ghose, D.: Sliding-mode guidance and control for all-aspect interceptors with terminal angle constraints. J. Guid. Control Dyn. **35**(4), 1230–1246 (2012)
18. Kumar, S.R., Rao, S., Ghose, D.: Nonsingular terminal sliding mode guidance with impact angle constraints. J. Guid. Control Dyn. **37**(4), 1114–1130 (2014)
19. Xiong, S.F., Wang, W.H., Liu, X.D., Wang, S., Chen, Z.Q.: Guidance law against maneuvering targets with intercept angle constraint. ISA Trans. **53**(4), 1332–1342 (2014)
20. Kumar, S.R., Ghose, D.: Impact time guidance for large heading errors using sliding mode control. IEEE Trans. Aerosp. Electron. Syst. **51**(4), 3123–3138 (2015)
21. Lee, J.I., Jeon, I.S., Tahk, M.J.: Guidance law to control impact time and angle. IEEE Trans. Aerosp. Electron. Syst. **43**(1), 301–310 (2007)
22. Harl, N., Balakrishnan, S.N.: Impact time and angle guidance with sliding mode control. IEEE Trans. Control Syst. Technol. **20**(6), 1436–1449 (2012)
23. Young, K.D., Utkin, V.I., Ozguner, U.: A control engineer's guide to sliding mode control. IEEE Trans. Control Syst. Technol. **7**(3), 328–342 (1999)
24. Cong, B.L., Chen, Z., Liu, X.D.: On adaptive sliding mode control without switching gain overestimation. Int. J. Robust Nonlinear Control **24**(3), 515–531 (2014)
25. Ryoo, C.K., Cho, H., Tahk, M.J.: Optimal guidance laws with terminal impact angle constraint. J. Guid. Control Dyn. **28**(4), 724–732 (2005)
26. Ryoo, C.K., Cho, H., Tahk, M.J.: Time-to-go weighted optimal guidance laws with impact angle constraints. IEEE Trans. Control Syst. Technol. **14**(3), 483–492 (2006)
27. Rao, S., Ghose, D.: Terminal impact angle constrained guidance laws using variable structure systems theory. IEEE Trans. Control Syst. Technol. **21**(6), 2350–2359 (2013)
28. Zheng, Q., Gao, L.Q., Gao, Z.Q.: On stability analysis of active disturbance rejection control for nonlinear time-varying plants with unknown dynamics. In: Proceedings of the 46th IEEE Conference on Decision and Control, New Orleans, LA, pp. 3501–3506 Dec. (2007)